

# An empirical criterion to classify T Tauri stars and substellar analogs using low-resolution optical spectroscopy

David Barrado y Navascués

*Laboratorio de Astrofísica Espacial y Física Fundamental, INTA, P.O. Box 50727, E-28080 Madrid, Spain*

barrado@laeff.esa.es

and

Eduardo L. Martín<sup>1</sup>

*Institute of Astronomy, University of Hawaii at Manoa, 2680 Woodlawn Drive, Honolulu, HI 96822, USA.*

## ABSTRACT

We have compiled and studied photometric and spectroscopic data published in the literature of several star forming regions and young open clusters (Orion, Taurus, IC348, Sco-Cen Complex, Chamaeleon I, TW Hya association,  $\sigma$  Orionis cluster, IC2391,  $\alpha$  Per cluster and the Pleiades). Our goal was to seek the definition of a simple empirical criterion to classify stars or brown dwarfs which are accreting matter from a disk on the sole basis of low-resolution optical spectroscopic data. We show that using  $H\alpha$  equivalent widths and spectral types we can statistically classify very young stars and brown dwarfs as classical T Tauri stars and substellar analogs. As a boundary between accreting and non accreting objects, we use the saturation limit of chromospheric activity at  $\text{Log}\{L(H\alpha)/L(\text{bol})\} = -3.3$  (determined in the open clusters). We discuss the uncertainties in the classification scheme due to the occurrence of flares. We have used this spectroscopic empirical criterion to classify objects found in the literature, and we compute the fraction of accreting objects in several star forming regions. The fraction of accreting objects appears to decrease from about 50% to about 5% from 1 Myr to 10 Myr for both stars and brown dwarfs.

*Subject headings:* open clusters and associations: (Orion, Taurus, IC 348, UpperSco,  $\rho$  Oph, Chamaeleon I, TW Hya association,  $\sigma$  Orionis, IC 2391,  $\alpha$  Per, the Pleiades) – Stars: low mass, brown dwarfs, pre-main-sequence, chromospheres, flare

## 1. Introduction

A classical T Tauri star (CTTS) is a pre-main sequence (PMS) star which presents a characteristic phenomenology which, in general, includes the following: i) An emission line spectrum, including, in the visible, lines such as the Balmer series with very intense  $H\alpha$ ; HeI  $D_1, D_2, D_3$  and HeI 6678 Å; CaII H & K and CaII infrared triplet at 8498, 8542 and 8662 Å; etcetera. These emission lines (in particular  $H\alpha$ ) are quite broad (sev-

eral hundred km/s at FWHM), and can present asymmetries. ii) The presence of forbidden – generally blue-shifted narrow– lines (for example, [O I]6300&6364, [N II]6458&6581, [S II]6717&6731). iii) Photospheric continuum excesses, specially in the ultraviolet, the blue part of the optical range and the infrared (Class II spectral energy distribution). Not all of them appear simultaneously.

There are different proposed criteria to define CTTS, and they do not always agree with each other. The simplest criterion is based on the equivalent width of  $H\alpha$  ( $W(H\alpha)$ ). Critical values between 5 and 20 Å have been put forward.

<sup>1</sup>also at Instituto de Astrofísica de Canarias, 38200 La Laguna, Spain

Martín (1998) suggested a dependence with the spectral type: 5 Å for spectral types earlier than M0, 10 Å for M0–M2, and 20 Å for later spectral types.

The canonical interpretation of CTTS phenomenology states that they possess a circumstellar disk, containing a significant fraction of the mass of the star, which is the source of the infrared excess, and a strong magnetosphere (see Appenzeller & Mundt 1989 for a review). Material from the disk would be magnetically accreted onto the star, in a channeled flux, creating a hot spot, the source of the continuum excesses in the blue side of the spectrum. The broad, asymmetric H $\alpha$  (or other hydrogen lines) is produced by this material falling from the disk. In general, for permitted lines, blue-shifted absorptions denote strong winds, whereas red-shifted absorptions indicate infalls. Finally, the forbidden lines are produced in outflows, which are –as this interpretation goes– jets perpendicular to the disk, and are driven by the accretion. For more details, see Shu et al. (1994), Hartmann et al. (1994) and Hartmann (1998).

Weak-line T Tauri stars (WTTS) lack most of the observational features of CTTS. They show H $\alpha$  in emission but with equivalent widths smaller than in the case of CTTS (Herbig & Bell 1988). Some WTTS show infrared excess, but not ultraviolet excess or optical veiling. Naked T Tauri stars (NTTS) are equivalent to the WTTS but without infrared excess (Walter 1986). It is assumed that WTTS are in a more advanced stage of their evolution, with no circumstellar accretion disks. Hence, the origin of the emission in H $\alpha$  should be purely chromospheric. WTTS are still very young (<10 Myr), and their interior has not reached a temperature hot enough to destroy lithium which burns at about  $2.5 \times 10^6$  K. Finally, post-T Tauri stars (PTTS) represent the subsequent PMS evolution of the previous two phases. Together with rapid rotation and high activity levels, they have already started the lithium depletion (Martín 1997, 1998).

Brown dwarfs (BD) are substellar objects which are unable to settle on the main sequence because their interior reaches a degenerate state (Hayashi & Nakano 1963; Kumar 1963). For solar metallicity, current models predict that the borderline between stars and BDs is at  $0.072 M_{\odot}$  (Burrows et al. 1997; Baraffe et al. 1998; Chabrier et al. 2000).

BDs are low-mass analogs to PMS stars because they are fully convective, gravitationally contracting objects. There is a continuity from the stellar to the substellar regime in a color-magnitude diagram, a continuous dwarf sequence. In fact, very low mass (VLM) stars need tens of billion of years to reach the MS (longer than the age of the Universe). Observationally, the substellar limit is located at spectral type of M6 in the Pleiades cluster (Martín et al. 1996). This spectral type boundary between stars and BDs is also used in the literature for very young ages (Luhman et al. 1998).

Since the discovery of the first confirmed BDs in the Pleiades cluster (Rebolo et al. 1995; Basri et al. 1996), an avalanche of discoveries and theoretical work has taken place. The standard formation mechanism of BDs is that they come from small cores produced by the fragmentation of molecular clouds –star formation does not know about the H-burning substellar limit. Recent theoretical work indicates that very small fragments can be produced by turbulence in molecular clouds (Padoan & Nordlund 2002). If BDs are formed in a similar manner as stars, it seems natural to expect that some very young BDs could share the same properties as CTTS. In particular, they could have circum-substellar disks with active accretion leading to an emission line spectrum and continuum excesses. In fact, during the last 2 years some initial reports indicate that a few of them, indeed, have disks (Martín et al. 2001a; Natta & Testi 2001; Natta et al. 2002; Testi et al. 2002; Jayawardhana et al. 2002ab, 2003ab; Barrado y Navascués et al. 2002, 2003; White & Basri 2003).

The main aim of this paper is to explore an empirical criterion based on low-resolution optical spectroscopy, which allows to identify accretion phenomena by distinguishing between CTTS, WTTS and their substellar analogs. We adopt the following definitions: substellar classical T Tauri analog (SCTTA), which is a substellar-mass object that shows emission lines indicative of active accretion similar to those observed in CTTSs; substellar weak-line T Tauri analog (SWTTA), which shows chromospheric line emission similar to that of WTTS. We find that SCTTAs and SWTTAs can be classified statistically from low-resolution optical spectroscopy using spectral types and  $W(\text{H}\alpha)$ . Another criterion, proposed by White & Basri (2003), is based on the width

of this line, but its application demands high resolution spectroscopy which is more difficult to obtain, particularly for intrinsically faint substellar objects. Our study extends the classical/weak-line T Tauri classification into the substellar regime. We have applied our criterion to derive the ratio of SCTTA/SWTTA in different star-forming regions. This ratio allows us to discuss the dependence of accretion on age, mass and location.

In section 2, we discuss some of the properties of the CTTS and WTTS population of very young clusters and star forming regions. It also presents an analysis of the  $H\alpha$  equivalent width as a the main empirical criterion to classify CTTS, WTTS, SCTTA and SWTTA. In Section 3, we compare the ratios of accretion in several star forming regions. Section 4 summarizes the results, stating the main conclusions.

## 2. $H\alpha$ equivalent width as an empirical criterion of accretion and chromospheric activity

### 2.1. Infrared excesses and $H\alpha$ emission in T Tauri stars

Both classical and weak-line T Tauri stars have been identified using near infrared color-color diagrams. We have collected  $H\alpha$  equivalent widths of T Tauri stars belonging to different star forming regions and very young clusters and compared them with the color excesses. These color excesses were computed using the measured color indices and spectral type, and the typical color indices corresponding to the spectral type, as listed by Bessell & Brett (1988), Kirkpatrick et al. (2000), and Leggett (1992) and Leggett et al. (2000, 2002).

Figure 1 illustrates one of these comparisons for stars in Taurus. Open and solid circles denote the location of weak-line and classical T Tauri stars, respectively. In this and other figures discussed below displaying  $W(H\alpha)$ , we have avoided objects which have been classified as classical or weak-line T Tauri stars or substellar analogs based on the  $W(H\alpha)$ , i.e., the displayed CTTS and SCTTA show either broad  $H\alpha$ , forbidden lines, strong infrared excesses, or veiling. All the data presented in this paper come from a large diversity of papers (see section 2.4 for references), and the corresponding spectra were collected at very different resolutions. This can translate into different val-

ues of the equivalent width for a given object (i.e., lower resolution tends to yield larger  $W(H\alpha)$  than high resolution spectroscopy). This is a caveat that has to be kept in mind through this and any other similar analysis.

In Figure 1, we display as short dashed lines two  $W(H\alpha)$  criteria used in the literature for classifying CTTS. Clearly, most of the CTTS are above the 20 Å threshold, whereas most of the WTTS have  $W(H\alpha) \leq 5$  Å. However, there is an area in between where the transition from WTTS to CTTS is not clear-cut. Part of the confusion arises from the fact that  $H\alpha$  emission can also be produced by chromospheric activity. Therefore, our next step is to study the  $H\alpha$  emission of active young stars.

### 2.2. The $H\alpha$ emission in young open clusters

Figure 2a displays the ratio between the  $H\alpha$  and the bolometric luminosities versus the spectral type for members of three young open clusters, namely the Pleiades, Alpha Per and IC2391. The age ranges are 80–125 Myr, 50–90 Myr, and 30–53 Myr for each of them, depending on the age dating technique: upper main-sequence isochrone fitting or lithium depletion at the substellar limit, respectively (Maeder & Mermilliod 1981; Meynet et al. 1993; Stauffer et al. 1998, 1999; Barrado y Navascués et al. 1999). The vertical, dotted lines delimit the age-dependent lithium gap in each cluster (see Barrado y Navascués & Stauffer 2003 and references therein). In order to convert  $H\alpha$  equivalent width into luminosity, we followed a similar procedure as the one described by Mohanty & Basri (2003). We computed fluxes corresponding to the continuum around 6563 Å –  $F_{cont}(H\alpha)$  – using theoretical models by Allard et al. (2001). We selected those having  $\log g=4.5$ , which correspond to ages between 50 and 100 Myr (Baraffe et al. 1998). In particular, we used “dusty” models for  $T_{eff} \leq 3900$  K and “NextGen” models for higher effective temperatures. We note that “NextGen” models are good enough down to  $T_{eff}=2500$  K (Martín et al. 2001b), but the predicted fluxes for both sets are very similar and they do not affect the results. Then, the flux of the  $H\alpha$  emission line was computed as  $F_{line}(H\alpha) = W(H\alpha) \times F_{cont}(H\alpha)$ . Finally, the ratio can be expressed as  $L(H\alpha)/L(bol) = F_{line}(H\alpha)/\sigma T_{eff}$ , where  $L(H\alpha)$  and  $L(bol)$  are the luminosity in the

H $\alpha$  line and the bolometric luminosity. This diagram clearly shows a maximum at -3.3, which it is essentially defined by low mass stars with M2-M4 spectral types. A similar diagram was obtained by Mohanty & Basri (2003) for mid-M and L field objects (see their figure 7). Besides H $\alpha$ , this saturation limit also occurs in other activity indicators such as the X-ray luminosity (Stauffer et al. 1994; Randich et al. 1996) or in H $\beta$  (Delfosse et al. 1998).

We have found that our saturation limit,  $\log \{L(H\alpha)/L(bol)\} = -3.3$ , derived from the young open clusters IC2391, Alpha Per and the Pleiades, is somewhat higher than the values obtained by Delfosse et al. (1998) and Mohanty & Basri (2003) in field mid-dM stars, and late M and L spectral type very low mass stars and BDs. Since the first group (cluster members) are, on average, younger, and they have larger radius (the ratio between the radii of a 0.072  $M_{\odot}$  at 100 and 500 Myr is 4.7, according to Baraffe et al. 1998 models), this difference suggests that there is an evolutionary component, perhaps related with size and/or surface gravity, in the saturation limit and, by extension, in the chromospheric activity in objects at the end of the dwarf sequence. A similar conclusion has been reached by Basri & Mohanty (2003).

Now, we are interested on observational quantities, in particular  $W(H\alpha)$ . Therefore, starting with this saturation limit, we have proceeded backward and derived the  $W(H\alpha)$  value for each spectral type which would correspond to it. Since we are trying to define a criterion for CTTS and SCTTA, which have maximum ages of about 10 Myr, we have used the atmosphere models corresponding to a gravity of  $\log g = 4.0$ . Figure 2b shows the measured  $W(H\alpha)$  of members (low mass stars and BDs) of these three young clusters. The bold-dotted line corresponds to the saturation limit at  $\log \{L(H\alpha)/L(bol)\} = -3.3$  dex. This criterion can be found in tabular form in Table 1. From now on, this criterion will be called the *saturation criterion*.

The dashed line in Figure 2b corresponds to the upper envelope of the  $W(H\alpha)$  for the clusters. For objects cooler than M5.5, the maximum  $W(H\alpha)$  measured is 20 Å. Note, however, that the data are sparse at the low mass end of these cluster sequences. For stars warmer than this spectral type, the behavior is pseudo-linear in a logarithmic scale. We have selected a fit which includes

all the measurements. This curve, which is purely empirical, will be called the young cluster *chromospheric criterion* from now on. The mathematical expression of this criterion is:

$$\log W(H\alpha) = 0.0893 \times Sp.Type - 4.5767 \quad (1)$$

where the spectral type O1 corresponds to 1, B1 to 11, A1 to 21, etcetera. This fit is valid between spectral types G5 and M5.5.

There is a clear tendency that the cooler the object, the larger the H $\alpha$  equivalent width, on average. The general reason for this trend is the decreasing photospheric luminosity at the wavelength of H-alpha as the temperature decreases (the so-called "contrast effect"; Basri & Marcy 1995). The quantitative behavior of the line strength, however, is not well understood. We adopt this upper envelope as the maximum emission due to chromospheric activity, without taking into account values measured during flares (known flares, such as that of PPI-15 detected by Basri & Martín (1999), have been excluded).

### 2.3. The H $\alpha$ emission in flare stars and field M and L objects

Figure 3 is as Figure 2, but in this case a comparison with flare stars is displayed (UV Cet type, crosses). The figure also includes cooler objects recently discovered by the 2MASS survey (Skrutskie et al. 1997), down to the L5 spectral type (plus symbols). Note the logarithmic scale in the y-axis.

The selected UV Cet sample comes from Gershberg et al. (1999). The IAU defines UV Cet variables as: "Dwarf stars of spectral classes dM3e-dM6e characterized by rare and very short flares with amplitudes from 1 mag to 6 mag. Maximum brightness (usually sharp) is attained in a few, or several tens of seconds after the commencement of the flare, total duration of the flare being equal to about ten to fifty minutes". A more general definition, which comes from Gershberg et al. (1999), is: "UV Cet-type variables are stars on the lower part of the main sequence which show phenomena inherent to the solar activity. The most manifestations of the solar activity are detected on such stars: sporadic flares, dark spots, variable emissions from chromospheres and coronae, radio, X-

ray and UV bursts.” Therefore, this definition includes the first one (all the stars in the first group should be in the second). The sample shown in Figure 3 is based on this definition.

Regarding the cooler sample, the data come from Kirkpatrick et al. (2000), Gizis et al. (2000); Reid et al. (2002); and Mohanty & Basri (2003). In addition, stars and BDs with variable  $H\alpha$ , mainly due to the presence of flares, are also included as arrows and labeled. The beginning and the end of each arrow represent the minimum and maximum  $H\alpha$  equivalent width ever recorded. The data come from Ruiz et al. (1990); Irwin et al. (1991); Eason et al. (1992); Basri & Marcy (1995), Kirkpatrick et al. (1995); Martín et al. (1996, 1999, 2001), Delfosse et al. (1997); Tinney et al. (1998), Tinney (1999); Gizis et al. (1999, 2000); Liebert et al. (1999, 2003); Reid et al. (1999, 2002); Hall (2002ab); Zapatero Osorio et al. (2002b); and Mohanty et al. (2003).

This figure includes two different curves. The first one (bold, dotted line), also in Figure 2, is the saturation criterion. The second curve, plotted as a thin-solid line, is the upper envelope of the flare stars and field very low mass stars and brown dwarfs, which defines the *flare criterion*.

As the visual inspection and the comparison with Figure 2 show, most of the flare stars do have  $H\alpha$  equivalent width which is less or equal than the upper limit defined by cluster stars. In any case, in order to establish the nature of an object with a strong  $H\alpha$  emission, several consecutive spectra should be collected, to check the possibility of a flare. This is an advisable strategy regardless the final goal, when acquiring spectra (i.e., splitting the total exposure time into three or four consecutive observations).

#### 2.4. $H\alpha$ in very young stellar associations

We have done the same exercise for several star forming regions and very young clusters, with ages in the range 1-10 Myr, and displayed  $H\alpha$  equivalent width against the spectral type. These results are depicted in Figure 4, which includes the Orion population (from Herbig & Bell 1988; Alcalá et al. 1996, 1998, 2000), Taurus (Briceño et al. 1993, 1998, 1999, 2002; Alencar & Basri 2001; Martín et al. 2001a; Luhman et al. 2003a; White & Basri 2003; Muzerolle et al. 2003) IC348 (Herbig 1998;

Luhman et al. 1999, 2003b; Muzerolle et al. 2003; Jayawardhana et al. 2003a), Sco-Cen-Lupus-Crux Complex, including the  $\rho$  Oph molecular cloud (Bouvier & Appenzeller 1992; Martín et al. 1998, 2004, in prep; Ardila et al. 2000; Jayawardhana et al. 2002a; Mamajek et al. 2002), Chamaeleon I (Guenther et al. 1997; Comerón et al. 2000; Saffe et al. 2003; Jayawardhana et al. 2003),  $\sigma$  Orionis cluster (Béjar et al. 1999; Barrado y Navascués et al. 2001, 2002, 2003; Zapatero Osorio et al. 2002a), and TW Hydra association –TWA– (Sterzik et al. 1999; Webb et al. 1999; Zuckerman et al. 2001; Gizis 2002; Mohanty et al. 2003).

In these figures, solid circles, small open circles and open triangles correspond to CTTS/SCTTA, WTTS/SWTTA and PTTS, respectively. These classifications are based on criteria that do not use the  $W(H\alpha)$ . Small crosses denote unclassified objects. Note the logarithmic scale in the y-axis. Stars and BDs with mid-infrared excesses (signpost of circumstellar disks) are indicated as large open circles. They were selected from Natta & Testi (2001), Natta et al. (2002), Testi et al. (2002), Comerón et al. (1998), and Jayawardhana et al. (2002b, 2003b). In the case of the  $\sigma$  Orionis cluster, the large solid and broken circles denote the location of cluster members with near infrared excesses (Barrado y Navascués et al. 2003). Large open squares correspond to objects with forbidden lines (Zapatero Osorio et al. 2002a; Muzerolle et al. 2003; Briceño et al. 1998; Barrado y Navascués et al. 2004, in prep.), which characterize outflows. The vertical dotted segment is located at the spectral type which divides the stellar from the substellar domain (for ages younger than  $\sim 100$  Myr). The bold, dotted curve corresponds to the saturation criterion to classify CTTSs and substellar analogs. Traditional criteria dividing between classical and weak-line T Tauri stars, such as the 5 or 20 Å limits (long-dashed horizontal lines), are also included. Note that these criteria do not describe the CTTS/WTTS phenomenology appropriately. The criterion proposed by Martín (1998), which depends on the spectral type, is more reliable. Our saturation criterion improves upon the previous ones and extends into the substellar domain.

## 2.5. A new empirical criterion to classify classical T Tauri stars and substellar analogs

When weighting together all the data and criteria presented in the sections above, we have noted that most CTTS have  $H\alpha$  equivalent widths larger than the characteristic values of older stars (i.e., cluster and field stars) even when these last ones are flaring. Our main goal is to define an empirical spectroscopic criterion to classify any object as accreting or non-accreting using solely low-resolution optical spectroscopy. The data clearly indicate that all stars and brown dwarfs, except the few exceptions –mostly having large variability–, that are located above the saturation criteria (the  $H\alpha$  equivalent width corresponding to  $\log \{L(H\alpha)/L(\text{bol})\} = -3.3$ ) are, indeed, accreting and, therefore, they can be classified as bona-fide CTTS and SCTTA. This is a rather restricting criterion: all objects above this line should be CTTS and SCTTA (except for very strong peaks of flare activity which are short lived and rare). Below this dividing line there could be objects with a low-level of accretion. Furthermore, we note that throughout this paper, we have used the measured equivalent widths, without any correction due to the veiling of the continuum. Therefore, true equivalent widths should be equal or larger for CTTS and SCTTAs than the measured values, and all or some of the accreting objects located below the saturation criterion might be, in fact, above it once the veiling correction is performed. Unfortunately, the data in the literature are incomplete and very inhomogeneous regarding the technique to derive the veiling, and we have opted for using the uncorrected values.

In order to make easier the visual inspection, and to compare our criterion with all the available data, we have included in Figure 5 the information displayed in Figures 4a-4h. Figure 5 also shows (solid line) the re-definition of the criterion proposed by Martín (1998), carried out by White & Basri (2003). Our proposed criterion has a sound physical basis: the maximum amount of energy which can be released in non-thermal processes by the chromosphere,  $\sim 5 \times 10^{-4}$  of the total energy. Objects exceeding this limit must have drawn it from other sources, such as accretion from a disk. This criterion is listed in Table 1, which contains the  $H\alpha$  equivalent width depending on the spectral

type.

As a conclusion, a moderate signal-to-noise ( $S/N \sim 35$ ), low resolution ( $R \sim 600$ ) spectrum is enough to detect most of the CTTS and SCTTA. There are exceptions, such as a post-T Tauri star belonging to the Sco-Cen complex, with  $W(H\alpha)$  larger than the saturation criterion. However, additional information, such as the lithium abundance measured in the stellar photosphere, is enough to disentangle this ambiguity (see Martín et al. 1997, 1998). Finally, some of the substellar objects with disks (detected via their infrared excesses or because of the presence of forbidden lines in their spectrum) do not satisfy the proposed saturation criterion. We conclude that the amount of material they are accreting should be relatively small when compared with more massive accretors. This might suggest, too, that the time scale for disk dissipation is smaller in brown dwarfs. The veiling might be affecting by a large amount their evolution, when compared with accreting stars. Therefore, besides the saturation criterion, additional information is very helpful to detect accretion in most of the substellar objects, such as  $W(\text{HeI}5876)$ ,  $W(\text{HeI}6678)$  or the ratios between the components of the CaII infrared triplet. Note, however, that they have  $H\alpha$  above the cluster chromospheric criterion, which equals  $20 \text{ \AA}$  in this region (objects cooler than M5.5).

## 3. Accretion frequency

We have made use of our empirical criterion – the saturation at  $\log \{L(H\alpha)/L(\text{bol})\} = -3.3$  – to determine the number of CTTS and substellar analogs in several star forming regions, and to compute the fraction of accretors (i.e., the fraction of objects harboring an active circumstellar or circum-substellar disk). Table 2 lists the name of the association or cluster, their age (including maximum and minimum values commonly quoted in the literature) and the fraction of accreting objects, as computed for several spectral ranges. Since the saturation criterion –based on the equivalent width of  $H\alpha$ – is very restrictive, the values compiled in the table can be considered as lower limits. Figure 6 displays, in a log-log plane, this information. In this figure, we depict in three different panels the fraction for stellar members (K3-M5.5) and substellar components (M5.5-L2

and M5.5-M7.5). The selection of the M5.5-M7.5 range responds to the need of avoiding biases due to incompleteness of the surveys. However, we do not appreciate any significant difference. We have selected the spectral type M5.5 as the substellar borderline based on theoretical models  $-1$  or  $10$  Myr isochrones– by Baraffe et al. (1998).

Although there are significant uncertainties due to poor statistics in some cases, ages derived in heterogeneous ways (different evolutionary tracks or methodology to convert theoretical parameters into observational quantities, see Stauffer et al. 1995), age spread within the association, and so on, the decline of the disk frequency seems to be linear.

The data suggest that the accretion disk lifetimes are similar in the substellar domain than for more massive objects. We note the low fraction of accreting stars found in Rho Oph, although this could be related to strong veiling which could diminish the measured  $H\alpha$  equivalent widths and, hence, the fraction of accretors estimated from  $H\alpha$ . Recent works (Muench et al. 2001, Haisch et al. 2001, Jayawardhana et al. 2003b, Liu et al. 2003) have derived the fraction of objects with disks using different techniques for these and other SFR. Although the ratios are systematically larger in those studies -it has been stated before that our fraction represents only a lower limit–, the trend of decreasing disk emission with age is similar to what we find. Thus,  $W(H\alpha)$  alone is adequate tool to study the frequency of accreting objects in clusters and star-forming regions.

#### 4. Final remarks

Based primarily on the saturation limit at  $\log \{L(H\alpha)/L(\text{bol})\} = -3.3$ , we have been able to establish an empirical criterion to distinguish between CTTS and WTTS, and we have extended it into the substellar domain. An schematic classification is shown in Figure 7. Four regions are defined in this figure. Region A is populated by CTTSs and their substellar analogs. They have  $W(H\alpha)$  above the line defined by the saturation (i.e., the origin cannot be chromospheric). Since the equivalent width values are very high, a moderate signal-to-noise, low resolution optical spectrum is enough to detect the presence of accretion. In region (B) classical, weak-line T Tauri and flar-

ing objects can be found. Most of the objects in this area should be BDs. In particular, all WTTS and CTTS with spectral type cooler than M5.5-M6. This area is delimited by the saturation criterion (up) and the maximum chromospheric activity measured in upper clusters (down).

Since there is a mixture of objects in region B, it is useful to obtain additional information about the objects.

b1.- Several consecutive spectra at moderate S/N, low resolution, can establish whether the object is flaring, since the  $H\alpha$  equivalent widths change very fast and with a very characteristic pattern.

b2.- Spectroscopy at  $R \sim 3000$  resolution ( $\Delta v = 100$  km/s) allows a rough study of the  $H\alpha$  line profile and width. In the case of very low mass stars and brown dwarfs, White & Basri (2003) have proposed  $\text{FWHM} = 270$  km/s as a criterion to establish the presence of accretion (i.e., CTTS/SCTTA).

b3.- At this resolution, the lithium feature at  $6708 \text{ \AA}$  can be detected ( $S/N \sim 35$ ). The lack of lithium denotes that the object is older than the time needed for disk dissipation ( $\sim 10$  Myr) and must have a mass larger than  $0.060 M_{\odot}$ .

b4.- Other lines and line ratios, measured in low or medium resolution spectra, such as those  $\text{HeI}5876$ ,  $\text{HeI}6677$  and  $\text{CaII IRT}$ , can differentiate between CTTS/SCTTA, WTTS/SWTTA, and older objects experiencing flares.

In region C there are classical, weak-line and post-T Tauri stars. The limits are the same as for region B, but in this case, this region is located at the warmer side of the diagram. Additional information that helps to classify objects in this regions includes spectroscopy with resolution  $R \sim 3000$ , which is enough to measure the width of the  $H\alpha$  line and use the 10% FWHM criterion, which allows the distinction between SCTTA and SWTTA. The lithium depletion or absence of it is an adequate tool for differentiating between T Tauri and post-T Tauri stars.

Region D is populated by cluster and field stars and BDs. This area also includes weak-line and post-T Tauri objects and is delimited by the upper envelope of the activity measured in young open clusters. Additional criteria to classify objects in region D include:

d1.- As in b1, several low resolution spectra are essential to detect a flare.

d2.- Again, a  $R \sim 3000$  spectrum suffices to detect

the lithium feature in an object with a spectral type later than about M0, and to measure the activity. Lithium equivalent width can be compared with the values shown by cluster members, weak-line and post-T Tauri stars and brown dwarfs.

d3.- Moderate resolution spectroscopy ( $R \geq 10,000$ ) provides measurements of the rotational velocity (*vsini*). Since there is a relationship between age and rotation (slower rotators being older for a given spectral type, Stauffer et al. 1987ab, 1989) for dwarfs earlier than about M6, this information characterizes, from the statistical point of view, the evolutionary status.

d4.- Finally, lithium equivalent widths can be measured in objects with spectral type earlier than M0 if a spectrum with resolution larger than  $R=10,000$  is available.

In all these four cases, the detection or lack of forbidden lines, as well as other permitted lines, as discussed in section 4.1, can put strong constraints on the CTTS/SCTTA or WTTS/SWTTA nature.

As a conclusion, by re-analyzing H $\alpha$  and lithium equivalent widths in members of several young open clusters and star forming regions, we have been able to define well-defined spectroscopic criterion based on the saturation limit for young open clusters, which can be used to statistically classify populations of stars and BDs in young open clusters and star-forming regions using low-resolution optical spectroscopy, which is efficiently obtained using multi-object spectrographs.

Financial support was provided by the Spanish “Programa Ramón y Cajal” and AYA2001-1124-CO2 programs. Partial funding was provided by the National Aeronautics and Space Administration (NASA) grant NAG5-9992 and National Science Foundation (NSF) grant AST-0205862. We are truly indebted to the referee, Gibor Basri, for his very useful comments.

## REFERENCES

- Alcalá, J.M., et al. 1996, A&A Suppl. Series 119, 7
- Alcalá, J.M., Chavarría, K.C., Terranegra, L., 1998, A&A 330, 1017
- Alcalá, J.M., Covino, E., Torres, G., Sterzik, M.F., Pfeiffer, M.J., Neuhäuser, R., 2000, A&A 353, 186
- Alencar, S.H.P., & Basri, G., 2000, AJ 119, 1881
- Allard, F., Hauschildt, P.H., Alexander, D.R., Tamanai, A., Sweintzer, A., 2001, ApJ 556, 357
- Appenzeller, I., Mundt, R., 1989, A&A Rev. 1, 291
- Ardila, D., Martín, E.L., Basri, G., 2000, AJ 120, 479
- Baraffe, I., Chabrier, G., Allard, F., Hauschildt, P. H., 1998, A&A, 337, 403
- Barrado y Navascués, D., Stauffer, J.R., Patten, B.M., 1999, ApJ Letters 522, 53
- Barrado y Navascués, D., Zapatero Osorio, M.R., Béjar, V.J.S. et al. 2001, A&A Letters 377, 9
- Barrado y Navascués, D., Zapatero Osorio, M.R., Martín, E.L., Béjar, V.J.S., Rebolo, R., Mundt, R., 2002, A&A Letters 393, 85
- Barrado y Navascués, D., Béjar, V.J.S., Mundt, R., Martín, E.L., Rebolo, R., Zapatero Osorio, M.R., Bailer-Jones, C.A.L., 2003, A&A, 404, 171
- Barrado y Navascués, D., & Stauffer, J.R., 2003, in “Brown Dwarfs”, IAU Symposium 211, Eds E.L. Martín, p. 155
- Barrado y Navascués, D., et al. 2004, ApJ in prep.
- Basri, G., Marcy, G.W., 1995, AJ 109, 762
- Basri, G., Marcy, G., Graham, J.R. 1996, ApJ 458, 600
- Basri, G., Martín, E.L., 1999, AJ 118, 2460
- Basri, G., Mohanty, S., 2003, in “Brown Dwarfs”, IAU Symposium 211, Eds E.L. Martín, p. 427
- Béjar, V. J. S., Zapatero Osorio, M. R., Rebolo, R., 1999, ApJ 521, 671
- Bessell, M.S., & Brett J.M., 1988. PASP 100, 1134
- Bouvier, J., Appenzeller, I., 1992, A&A Suppl. Series 92, 491



- Briceño, C., Calvet, N., Gomez, M., Hartmann, L.W., Kenyon, S.J., Whitney, B.A., 1993, *PASP* 105, 686
- Briceño, C., Hartmann, L., Stauffer, J.R., Martín, E. L., 1998, *AJ* 115, 2074
- Briceño, C., Calvet, N., Kenyon, S.J., Hartmann, L., 1999, *AJ* 118, 1354
- Briceño, C., Luhman, K.L., Hartmann, L., Stauffer, J.R., Kirckpatrick, J.D., 2002, *ApJ* 580, 312
- Burrow, A., et al. 1997, *ApJ* 491, 856
- Chabrier, G., Baraffe, I., Allard, F., Hauschildt, P., 2000, *ApJ*, 542, L119.
- Comerón, F., Rieke, G.H., Claes, P., Torra, J., Laureijs, R.J., 1998, *A&A* 335, 522
- Comerón, F., Neuhüser, R., Kaas, A.A., 2000, *A&A* 359, 269
- Delfosse, X., Tinney, C.G., Forveille, T., et al. 1997, *A&A Letters* 327, 25
- Delfosse, X., Forveille, T., Perrier, C., Mayor, M., 1998, *A&A* 331, 581
- Eason, E., Giampapa, M.S., Radick, R.R., Worden, S.P., Hege, E.K., 1992, *AJ* 104, 1161
- Gershberg, R.E., Katsova, M.M., Lovkaya, M.N., Terebizh, A.V., Shakhovskaya, N.I., 1999, *A&A Suppl.Series* 139, 555
- Gizis, J.E., Reid, I.N., Monet, D.G., 1999, *AJ* 118, 997
- Gizis, J.E., Monet, D.G., Reid, I.N., Kirkpatrick, J.D., Liebert, J., Williams, R.J., 2000, *AJ* 120, 1085
- Gizis, J.E., 2002, *ApJ* 575, 484
- Guenther, E.W., Emerson J.P., 1997, *A&A* 321, 803
- Haisch, K.E., Lada, E.A., Lada, C.J., 2001, *ApJ Letters* 553, 153
- Hall, P.B., 2002, *ApJ Letters* 580, 77
- Hall, P.B., 2002, *ApJ Letters* 564, 89
- Hartmann, L., Hewett, R., Calvet, N., 1994, *ApJ* 426, 669
- Hartmann, L., 1998, "Accretion processes in star formation", Cambridge University Press.
- Hayashi, C., & Nakano, T. 1963, *Progr. Theor. Phys.*, 30, 460
- Herbig, G.H., Bell, K.R., 1988, *Lick Observatory Bulletin*, Lick Observatory
- Herbig, G.H., 1998, *ApJ* 497, 736
- Irwin, M., McMahon, R.G., Reid, N., 1991 *MNRAS* 252, 61
- Jayawardhana, R., Mohanty, S., Basri, G., 2002a, *ApJ Letters* 578, 141
- Jayawardhana, R., Holland, W.S., Kalas, P., Greaves, J.S., Dent, W.R.F., Wyatt, M.C., Marcy, G.W., 2002b, *ApJ Letters* 570, 93
- Jayawardhana, R., Mohanty, S., Basri, G., 2003a, *ApJ* 592, 282
- Jayawardhana, R., Ardila, D.R., Stelzer, B., Haisch, K.E., 2003b, in press
- Kenyon, S.J., Hartmann, L., 1995, *ApJ Suppl.Series* 101, 117
- Kirkpatrick, D., Henry, T.J., Simons, D.A., 1995, *AJ* 109, 797
- Kirkpatrick, D., Reid, I.N., Liebert, J., Gizis, J.E., Burgasser, A. J., Monet, D.G., Dahn, C.C., Nelson, B., Williams, R.J., 2000, *AJ* 120, 447
- Kumar, S.S., 1963, *ApJ* 137, 1121
- Leggett, S.K., 1992, *ApJ Suppl. Series* 82, 351
- Leggett, S.K., Allard, F., Dahn, C., Hauschildt, P. H., Kerr, T. H., Rayner, J. 2000, *ApJ* 535, 965
- Leggett, S.K., Golimowski, D.A., Fan, X., et al. 2002, *ApJ* 564, 452
- Liebert, J., Kirkpatrick, J.D., Reid, I.N., Fisher, M.D., 1999, *ApJ* 519, 345
- Liebert, J., Kirkpatrick, J.D., Cruz, K.L., Reid, I.N., Burgasser, A., Tinney, C.G., Gizis, J.E., 2003, *AJ* 125, 343
- Liu, M.C., Najita, J., Tokunaga, A.T., 2003, *ApJ* 585, 372

- Luhman, K.L., Briceño, C., Rieke, G. H., Hartmann, L., 1998, ApJ, 493, 909
- Luhman, K.L. 1999, ApJ, 525, 466
- Luhman, K.L., Briceño, C., Stauffer, J.R., Hartmann, L., Barrado y Navascués, D., Caldwell, N., 2003a, ApJ, 590, 348
- Luhman, K.L., Stauffer, J.R., Muench, A.A., Rieke, G.H., Lada, E.A., Bouvier, J., Lada, C.J., 2003b, ApJ, in press
- Maeder, A., Mermilliod, J.-C., 1981, A&A 93, 136
- Mamajek, E.E., Meyer, M.R., Liebert, J., 2002, AJ 124, 1670
- Martín, E.L., Rebolo, R., Zapatero Osorio, M. R. 1996, ApJ 469, 706
- Martín, E.L., 1997, A&A 321, 492
- Martín, E. L., 1998, AJ 115, 351
- Martín, E. L., Montmerle, T., Gregorio-Hetem, J., Casanova, S., 1998, MNRAS 300, 733
- Martín, E. L., Delfosse, X., Basri, G., Goldman, B., Forveille, T., Zapatero Osorio, M.R., 1999, AJ, 118, 2466
- Martín, E.L., Ardila, D., 2001, AJ 121, 2758
- Martín, E.L., Dougados, C., Magnier, E., Ménard, F., Magazzù, A., Cuillandre, J.-C., Delfosse, X., 2001a, ApJ Letters 561, 195
- Martín, E.L., Zapatero Osorio, M.R., Barrado y Navascués, D., Béjar, V.J.S., Rebolo, R., 2001b, ApJ Letters 558, 117
- Meynet, G., Mermilliod, J.-C., Maeder, A, 1991, A&A Suppl. Series 98, 477
- Mohanty, S., Basri, G., 2003, ApJ 583, 451
- Mohanty, S., Jayawardhana, R., Barrado y Navascués, D., 2003, ApJ Letters, in press
- Muench, A.A., Alves, J., Lada, C.J., Lada, E.A., 2001 ApJ Letters 558, 51
- Muzerolle, J., Hillenbrand, L., Calvet, N., Briceño, C., Hartmann, L. 2003, ApJ, 592, 266
- Natta, A., Testi, L., 2001, A&A Letters, 376, 22
- Natta, A., Testi, L., Comerón, F., Oliva, E., D'Antona, F., Baffa, C., Comoretto, G., Genari, S., 2002, A&A 393, 597
- Padoan, P., & Nordlund, Å., 2002, ApJ 576, 870
- Randich, S., Schmitt, J.H.M.M., Prosser, C.F., Stauffer, J.R., 1996, A&A 305, 785
- Rebolo, R., Zapatero Osorio, M.R., Martín, E.L., 1995, Nature 377, 129
- Reid, I.N., Kirkpatrick, J.D., Gizis, J.E., Liebert, J., 1999, ApJ Letters 527, 105
- Reid, I.N., Kirkpatrick, J.D., Liebert, J., Gizis, J.E., Dahn, C.C., Monet, D.G., 2002, AJ 124, 519
- Ruiz, M.T., Anguita, C., Maza, J., Roth, M., 1990, AJ 100, 1270
- Saffe, C., Gomez, M., Randich, S., Mardones, D., Caselli, P., Persi, P., Racca, G., 2003, A&A, in press
- Shu, F., Najita, J., Ruden, S. P., Lizano, S., 1994, ApJ 429 808
- Skrutskie, M. F., et al. in "The Impact of Large Scale Near-IR Sky Surveys", eds. F. Garzon et al., p. 25. Dordrecht: Kluwer Academic Publishing Company, 1997
- Stauffer, J.R., Hartmann, L.W., Latham, D.W., 1987a, ApJ Letters, 320, 51
- Stauffer, J.R., Hartmann, L.W., 1987b, ApJ 318, 337
- Stauffer, J.R., Hartmann, L.W., Jones B.F., 1989, ApJ 346, 160
- Stauffer, J.R., Caillault, J.P., Gagne, M., Prosser, C.F., Hartmann, L.W., 1994, ApJ Suppl. Series 91, 625
- Stauffer, J.R., Hartmann L., Barrado y Navascués D., 1995, ApJ 454, 910
- Stauffer, J.R., Schultz, G., Kirkpatrick, J.D., 1998, ApJ Letters 499, 199
- Stauffer, J.R., Barrado y Navascués, D., Bouvier, J., et al. 1999, ApJ 517, 219

- Sterzik, M.F., Alcalá, J.M., Covino, E., Petr, M.G., 1999, A&A Letters 346, 41
- Testi, L., Natta, A., Oliva, E., D'Antona, F., Comerón, F., Baffa, C., Comoretto, G., Genari, S., 2002, ApJ Letters 571, 155
- Tinney, C.G, Reid, I.N., 1998, MNRAS 301, 1031
- Tinney, C.G., 1999, MNRAS 269, 42
- Walter F.M. 1986, PASP, 98, 1100
- Webb, R.A., Zuckerman, B., Platais, I., Patience, J., White, R.J., Schwartz, M.J., McCarthy, C., 1999, ApJ Letters 512, 63
- White, R.J., & Basri, G., 2003, ApJ 582, 1109
- Zapatero Osorio, M.R., Béjar, V.J.S., Pavlenko, Ya., Rebolo, R., Allende Prieto, C., Martín, E.L., García López, R.J., 2002a, A&A 384, 937.
- Zapatero Osorio, M.R., Béjar, V.J.S., Martín, E.L., Barrado y Navascués, D., Rebolo, R. 2002b, ApJ Letters 569, 99
- Zuckerman, B., Webb, R.A., Schwartz, M., Becklin, E.E., 2001, ApJ Letters 549, 233

Table 1: CTTS criterion, expressed in equivalent widths, as derived from the saturation limit at  $\log \{L(\text{H}\alpha)/L(\text{bol})\}=-3.3$

Sp.Type	W(H $\alpha$ ) ( $\text{\AA}$ )
K0	3.9
K1	3.9
K2	4.0
K3	4.1
K4	4.4
K5	5.1
K6	5.9
K7	6.6
K8	7.2
K9	7.8
M0	8.7
M1	10.1
M2	11.2
M3	12.2
M4	14.7
M5	18.0
M6	24.1
M7	41.9
M8	53.0
M9	87.9
L0	148.2
L1	190.4
L2	279.6
L3	328.9
L4	436.4
L5	698.3

Table 2: Fraction of CTT stars and substellar analogs, in percentage. Inside the parenthesis, we list the number of accretors versus the total number of members ( $N/total$ ). Errors have been computed as  $\sqrt{N}/total$ .

SFR	Age			K3-M5.5	M5.5-L2	M5.5-M75
	Min.	Ave.	Max	(%)	(%)	(%)
	(Myr)					
Orion	0.5	1	1.5	68.3 ± 5.6 (151/221)	50.0 (1/2)	50.0 (1/2)
RhoOph	0.5	1	1.5	24.4 ± 5.2 (22/90)	20.0 ± 19.99 (1/5)	50.0 (1/2)
Taurus	1	1.5	2	52.9 ± 6.1 (93/158)	50.0 ± 12.9 (15/30)	45.5 ± 14.4 (10/22)
IC348	1	2	3	30.6 ± 4.4 (48/157)	40.0 ± 8.9 (20/50)	41.5 ± 10.1 (17/41)
ChaI	1	2	3	53.3 ± 13.3 (16/30)	25.0 ± 12.5 (4/16)	28.6 ± 14.3 (4/14)
SOri	2	5	8	25.0 ± 9.4 (7/28)	13.9 ± 6.2 (5/36)	14.5 ± 8.2 (3/21)
UpSco	3	5	12	14.4 ± 5.7 (4/35)	16.3 ± 6.2 (7/43)	13.5 ± 6.0 (5/37)
TWA	5	10	15	10.7 ± 6.1 (3/28)	7.1 ± 7.09 (1/14)	0.0 (0/6)

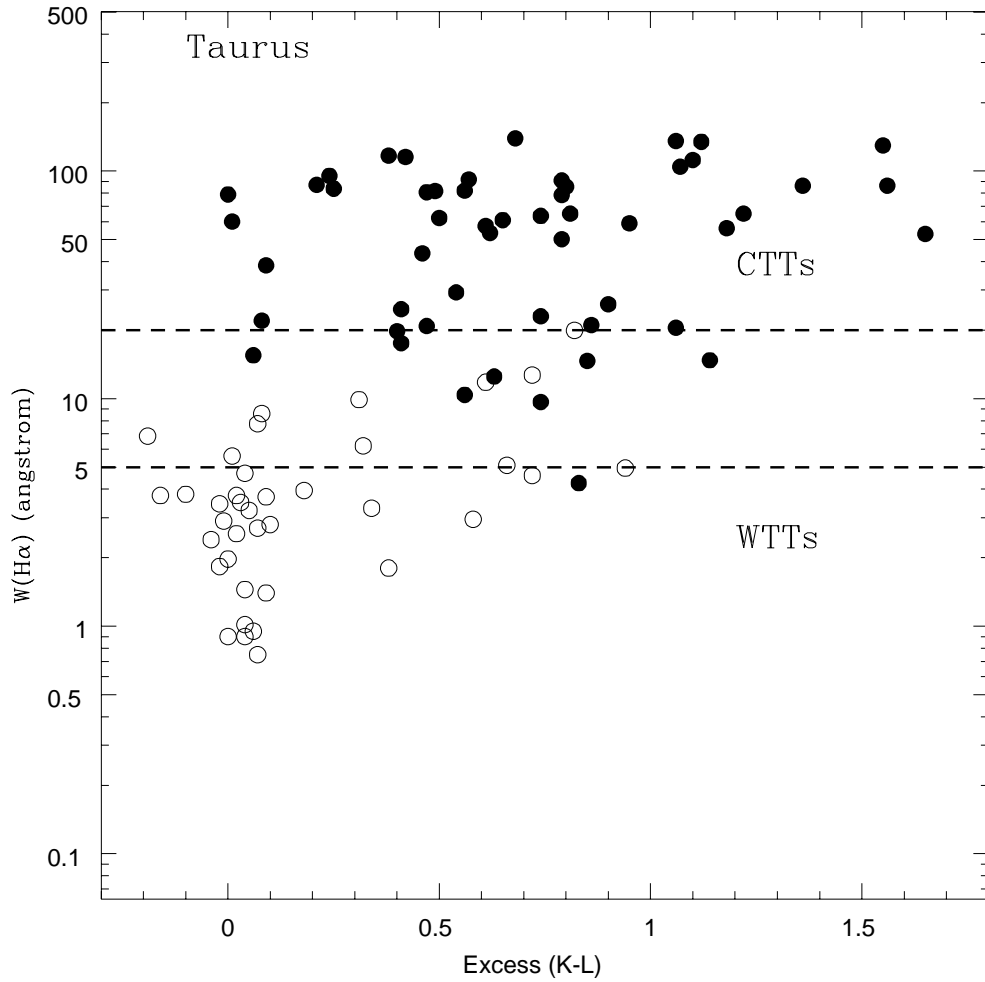


Fig. 1.— Equivalent width of  $H\alpha$  –logarithmic scale– against the color excess for the Taurus population (after Kenyon & Hartmann 1995). Classical and weak-line T Tauri are shown as solid and open circles, respectively. The two dashed lines delimit the areas for these two types of objects, based on the  $H\alpha$  emission.

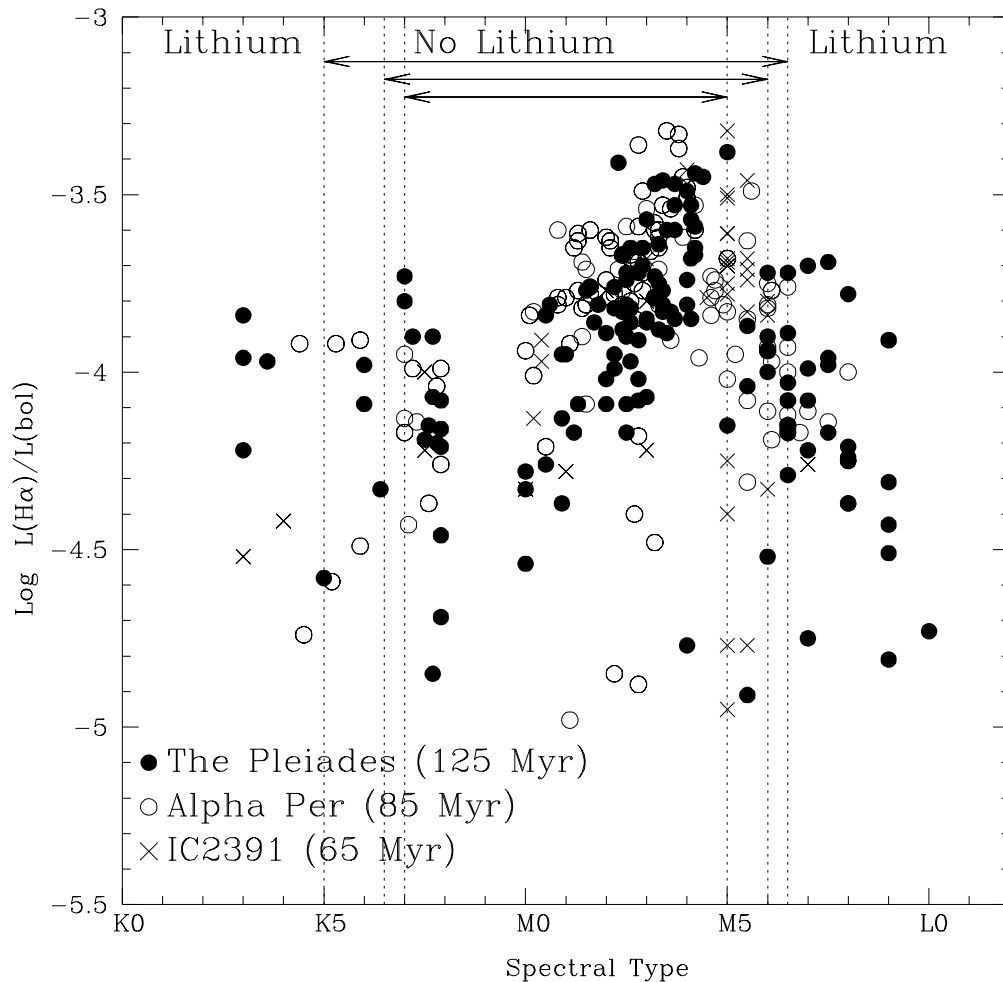


Fig. 2.— **a** Ratio between the  $H\alpha$  and the bolometric luminosities versus the spectral type for several young open clusters: the Pleiades (80-120 Myr), Alpha Per (50-90 Myr), and IC2391 (30-55 Myr). The vertical, dotted lines delimit the location of the spectral type ranges where the lithium has been preserved or depleted. **b** Same as panel a,  $H\alpha$  equivalent widths are plotted in the y-axis. The dashed segments correspond to the upper envelope of the  $W(H\alpha)$  for these three clusters (i.e., the maximum emission due to chromospheric activity). The bold, dotted curve is the saturation limit at  $\log \{L(H\alpha)/L(\text{bol})\} = -3.3$ . Note the linear scale in the y-axis.

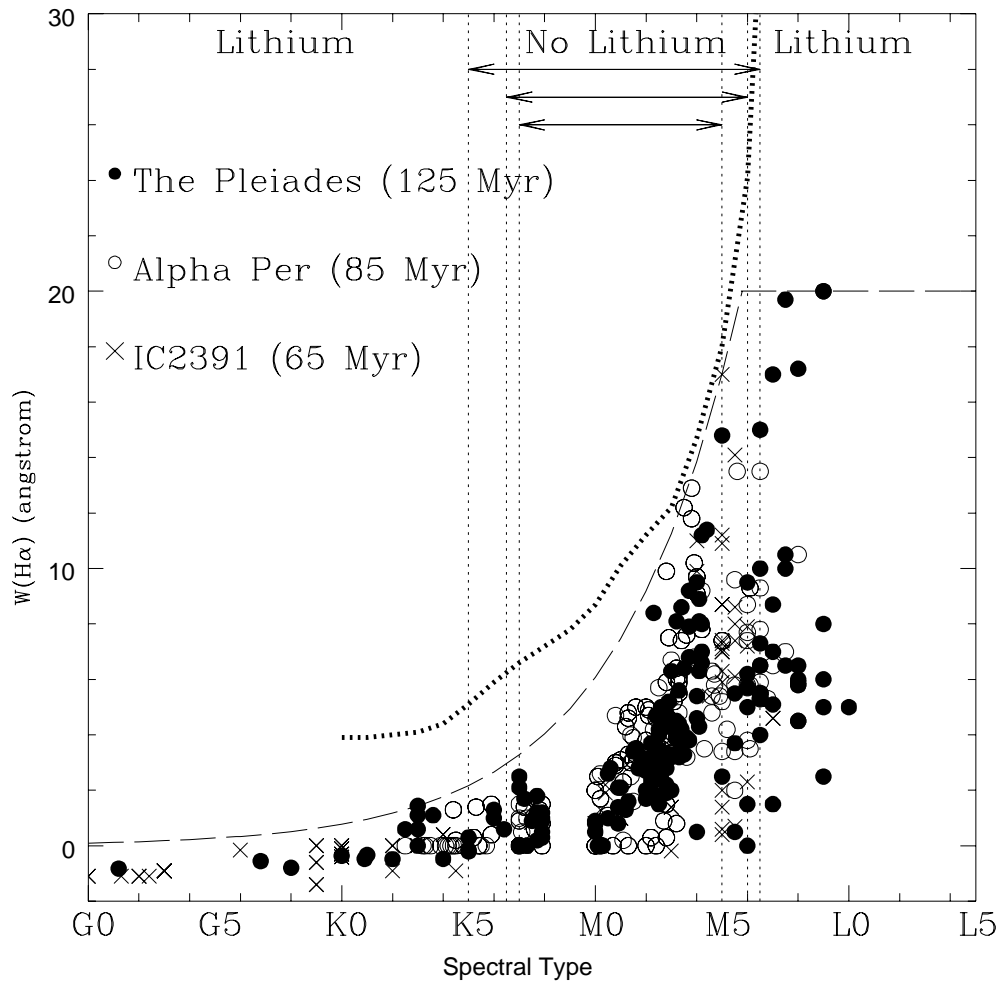


Fig. 2.— (continue)



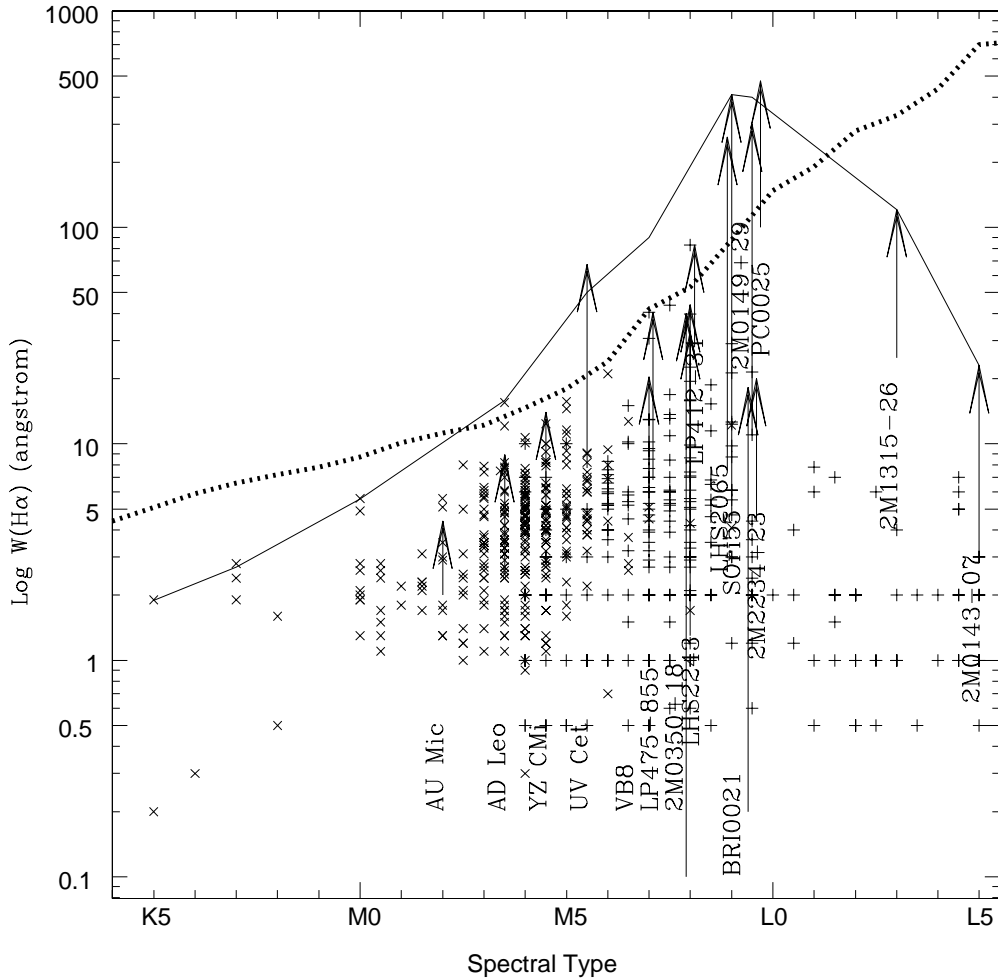


Fig. 3.—  $H\alpha$  equivalent widths for UV Cet stars (crosses, after Gershberg et al. 1999) and M and L objects, both very low mass stars and BDs, from 2MASS (plus signs, from Kirkpatrick et al. 2000; Gizis et al. 2002; Reid et al. 2002; Mohanty et al. 2003). Data corresponding to flares of several very active stars are also displayed as arrows. The thin solid curve corresponds to the upper envelope of flare stars and field object (i.e., the maximum emission for the flare of variable objects). The dotted, thick curve is the saturation limit. Note that most late M and L objects only have  $W(H\alpha)$  upper limits.

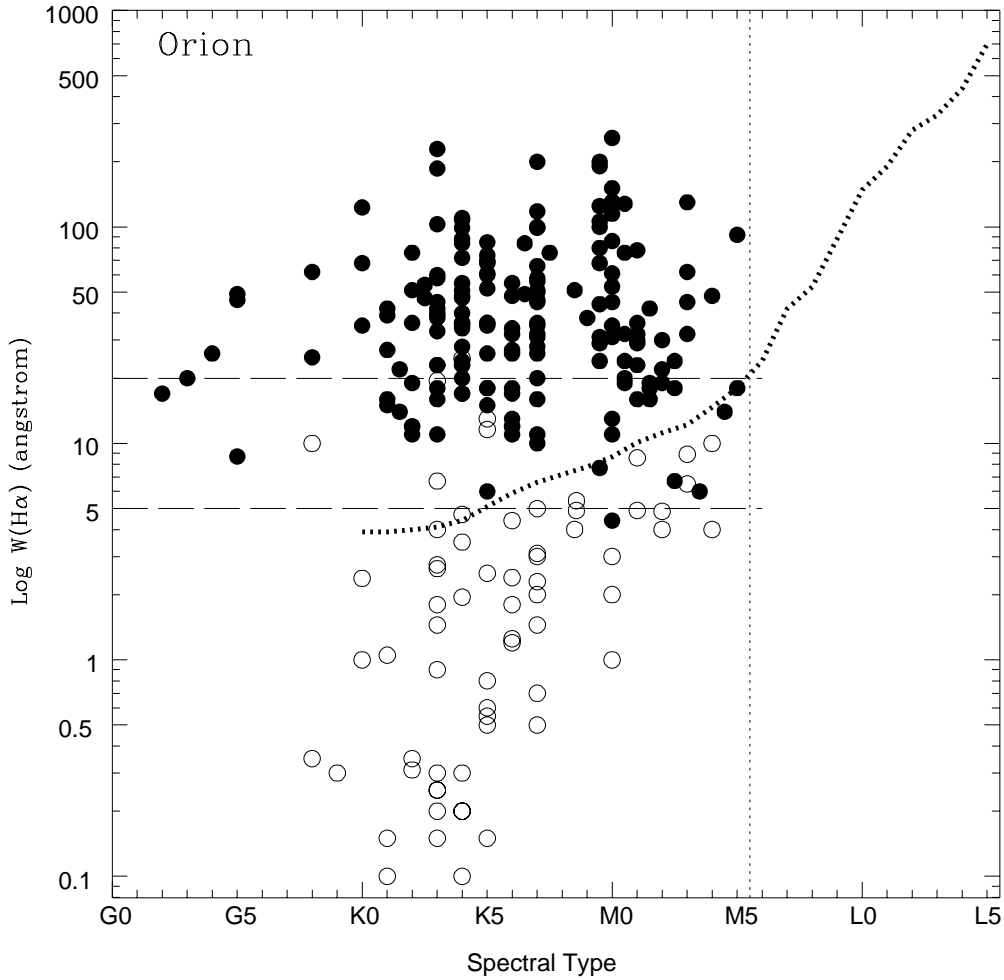


Fig. 4.— H $\alpha$  equivalent widths for several star forming regions: Orion population, Rho Oph, Taurus, IC348, ChaI,  $\sigma$  Orionis cluster, UpperSco, and the TW Hya association (see text for sources). Solid circles correspond to CTTS, open circles represent WTT stars and open triangles locate the position in the diagram of post-T Tauri. Objects with no classification are shown as crosses. Large open circles represent objects with mid-IR excesses. In the case of the  $\sigma$  Orionis cluster, the same symbols depict objects with near IR excesses (broken circles have possible excesses). Finally, large open squares denote objects with forbidden lines in their spectrum. The dotted, bold curve is the saturation criterion, whereas two previously proposed criteria (5 and 20 Å) to separate CTTS and WTTs (see section 3.4) are included as long-dashed, thin horizontal segments. The vertical dotted segment denotes the location of the substellar frontier for 100 Myr (i.e., longer than the expected lifetime of any circumstellar disk).

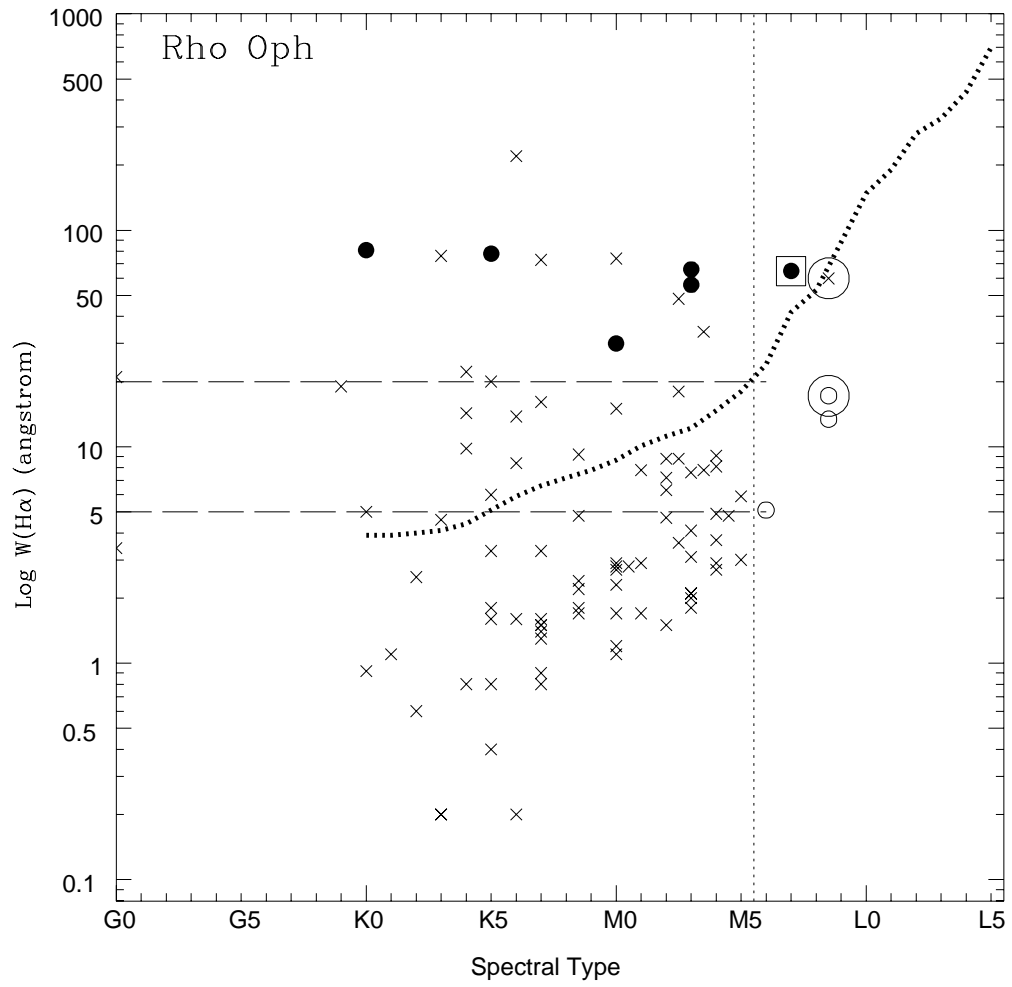


Fig. 4.— (continue)

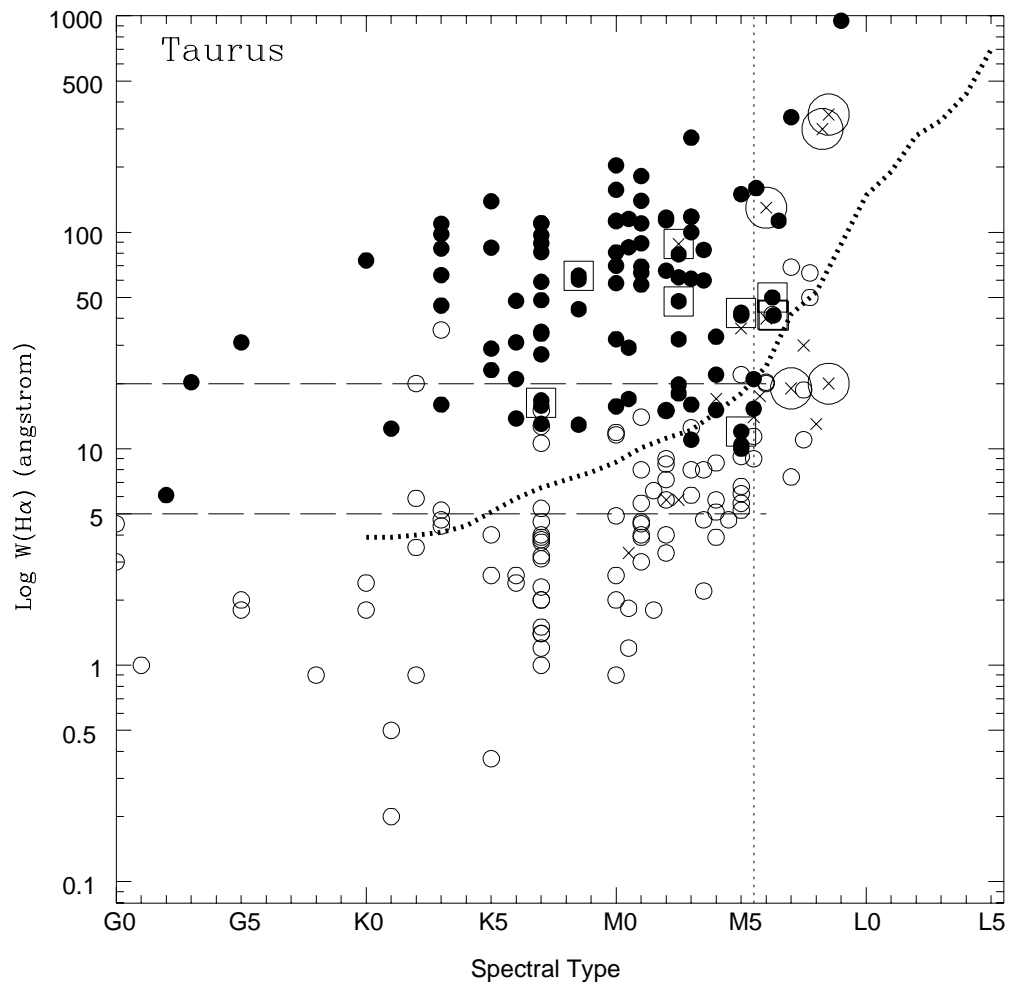


Fig. 4.— (continue)

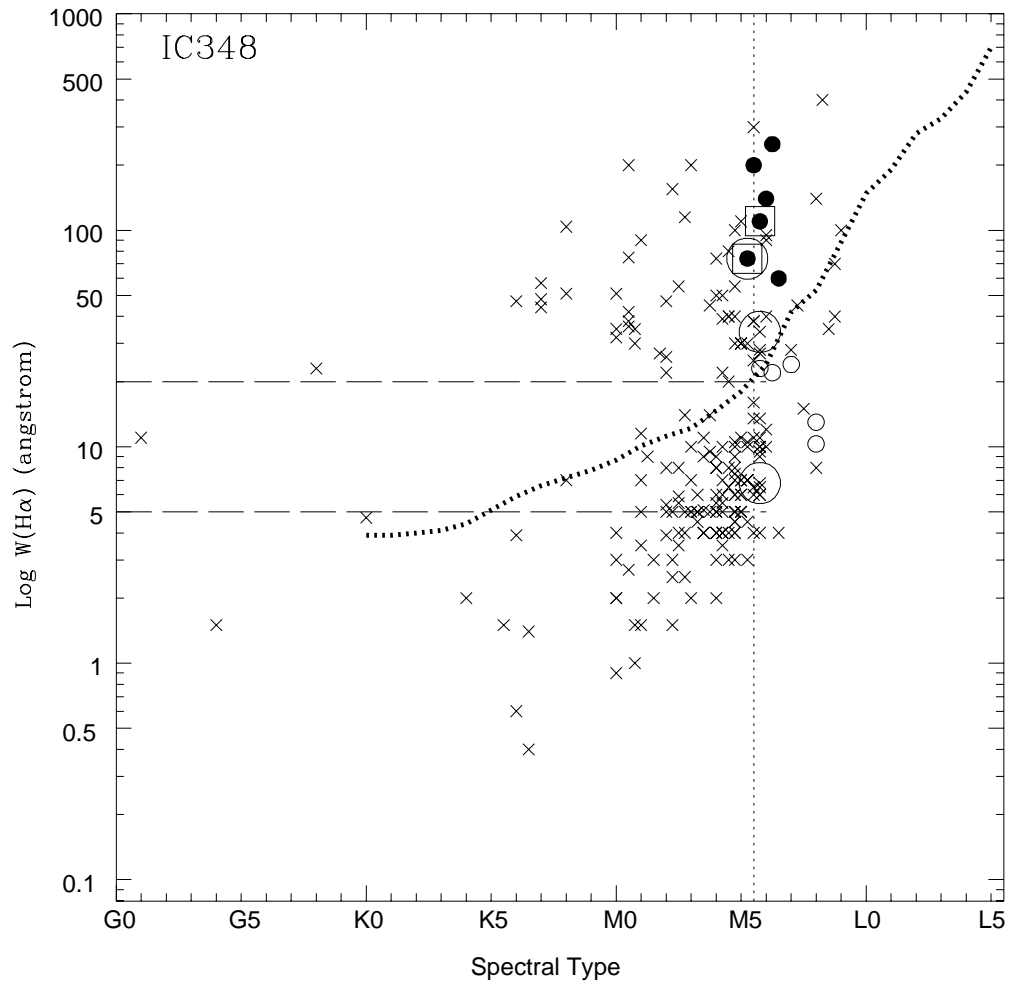


Fig. 4.— (continue)

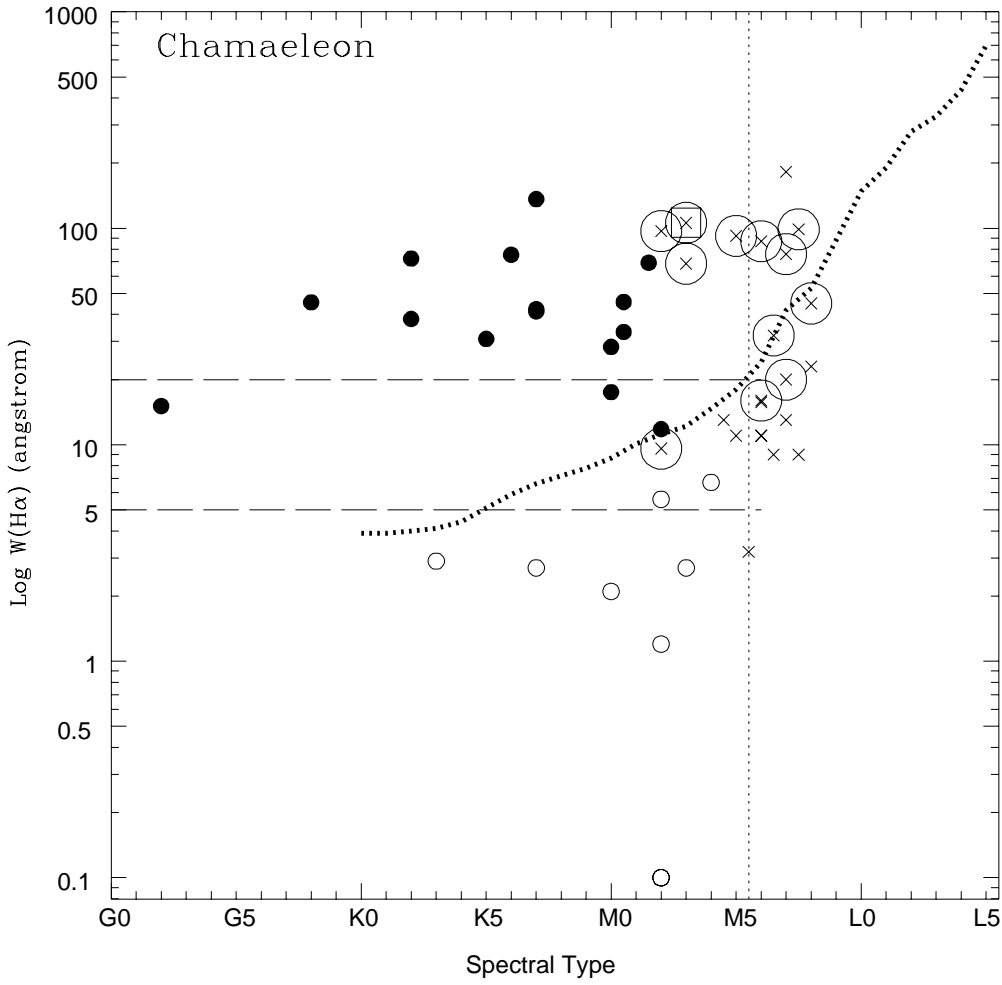


Fig. 4.— (continue)

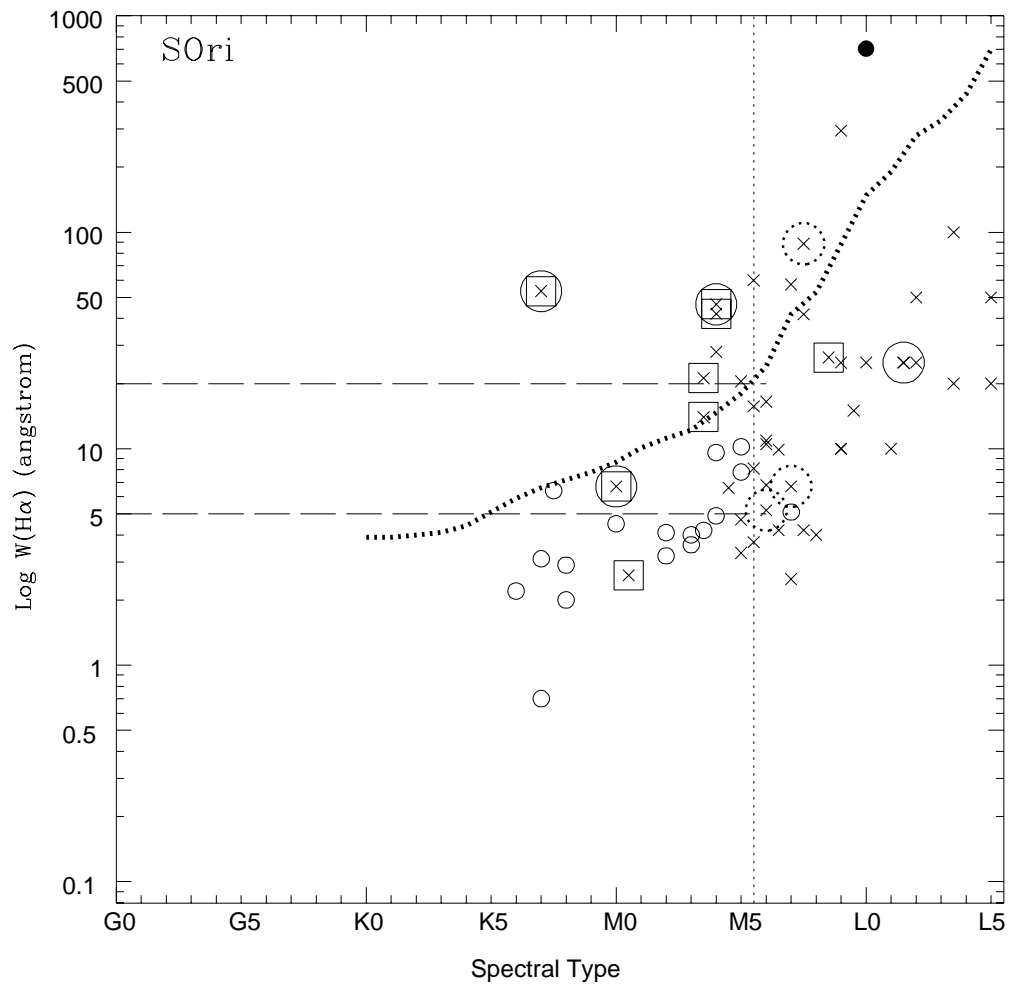


Fig. 4.— (continue)

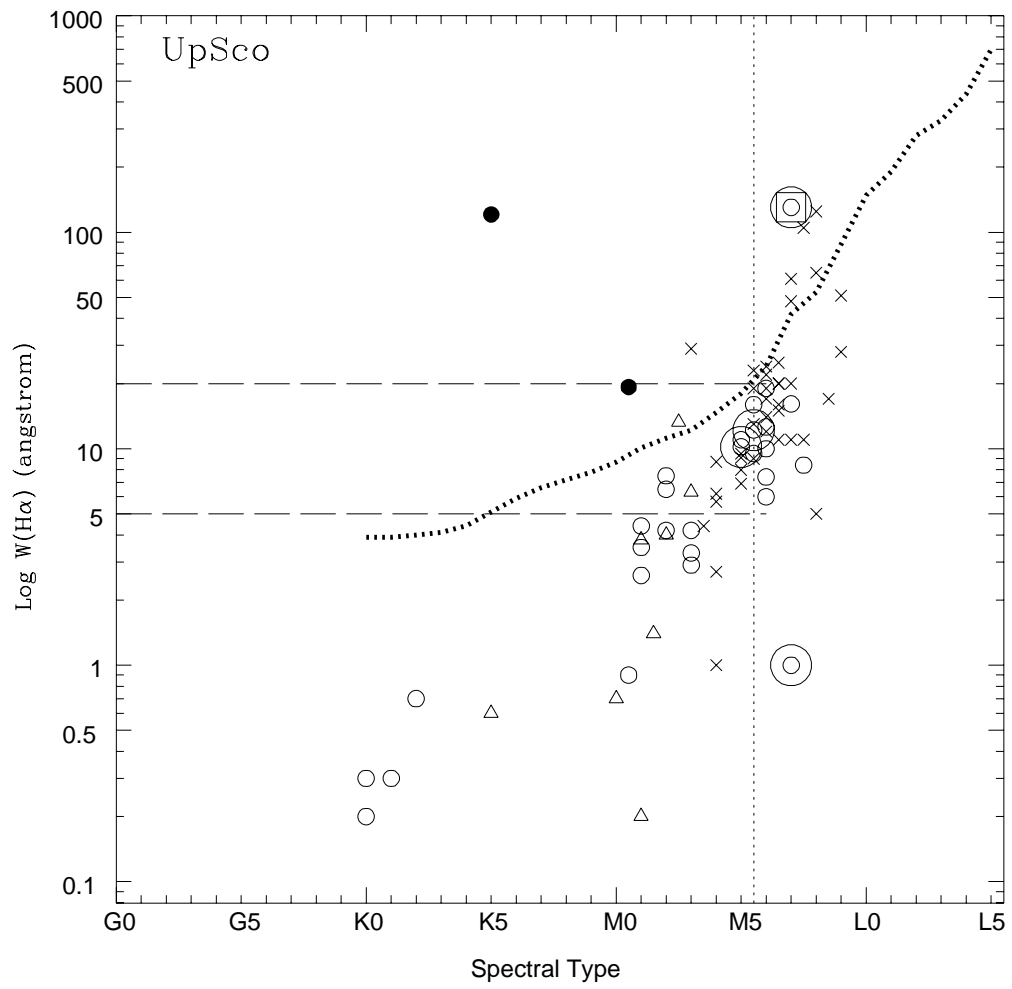


Fig. 4.— (continue)



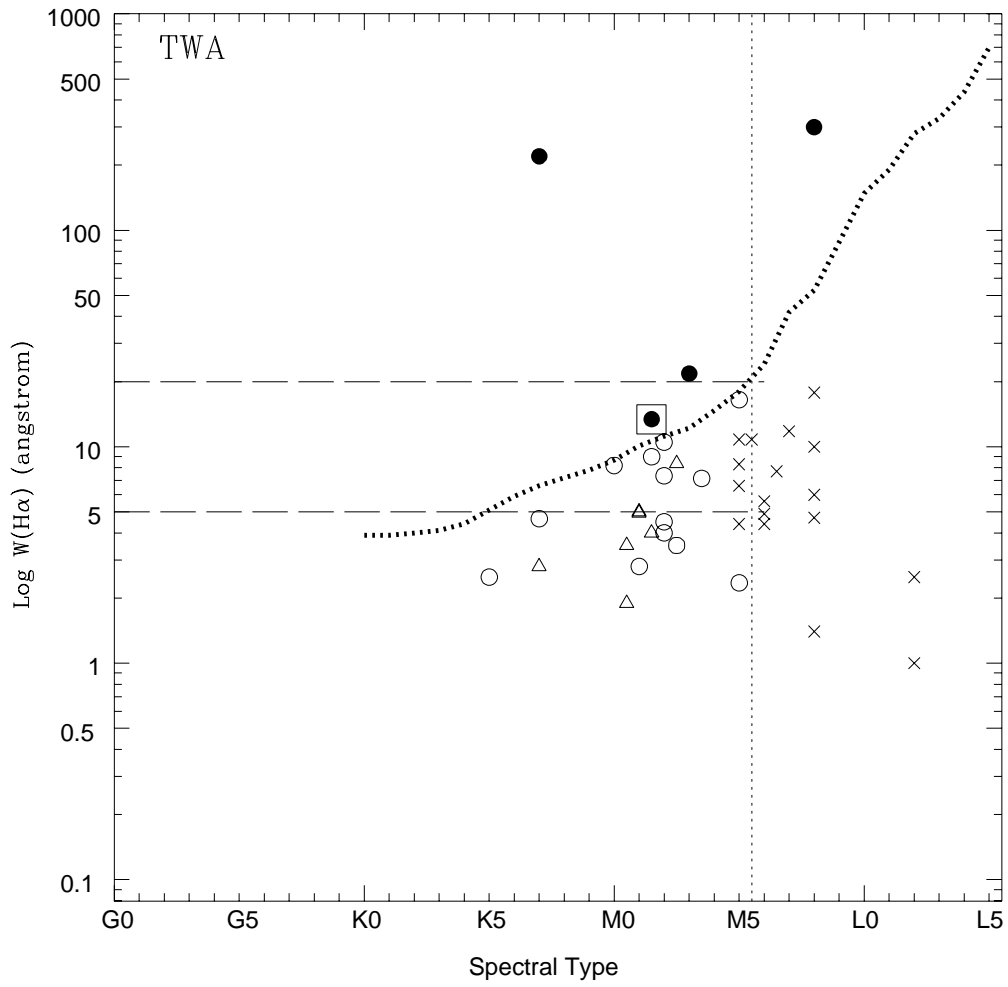


Fig. 4.— (continue)

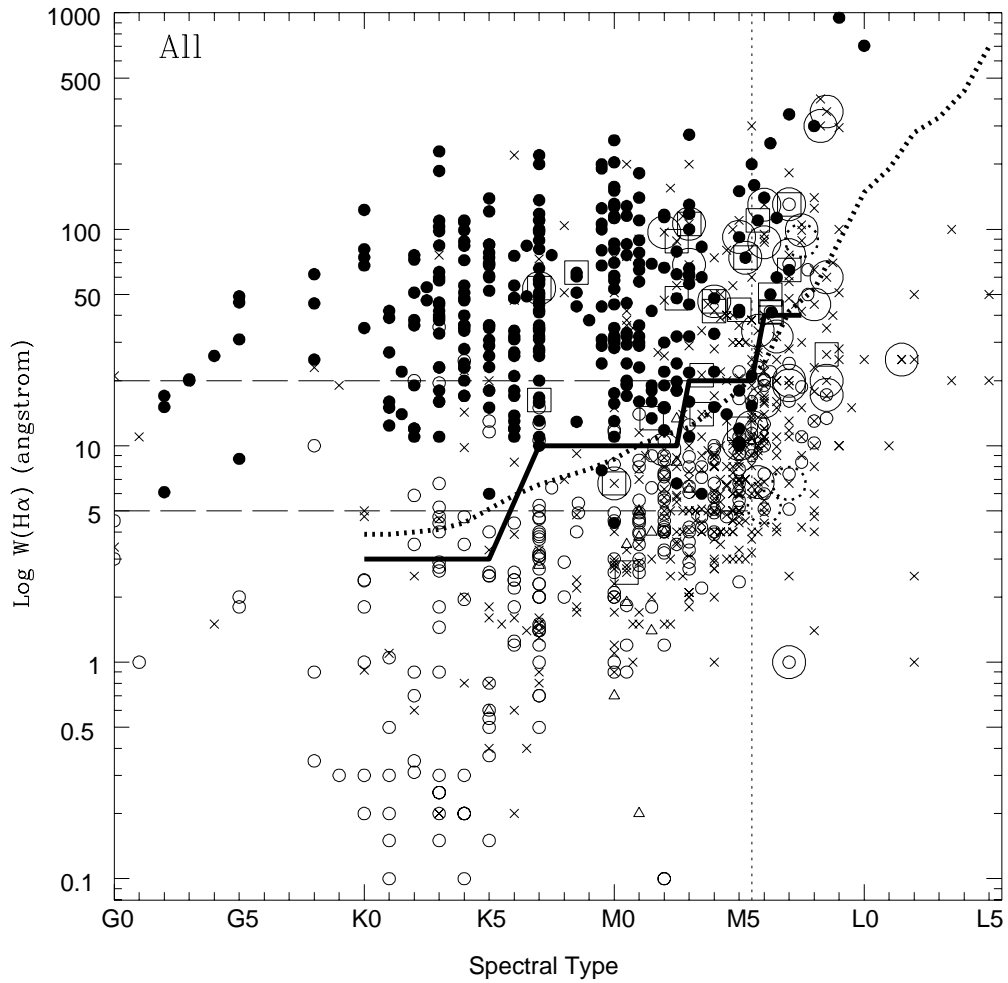


Fig. 5.— All data corresponding to the previous eight very young stellar associations. Labels as in Figure 4. We have also added the criterion defined by White & Basri (2003) as a solid line.

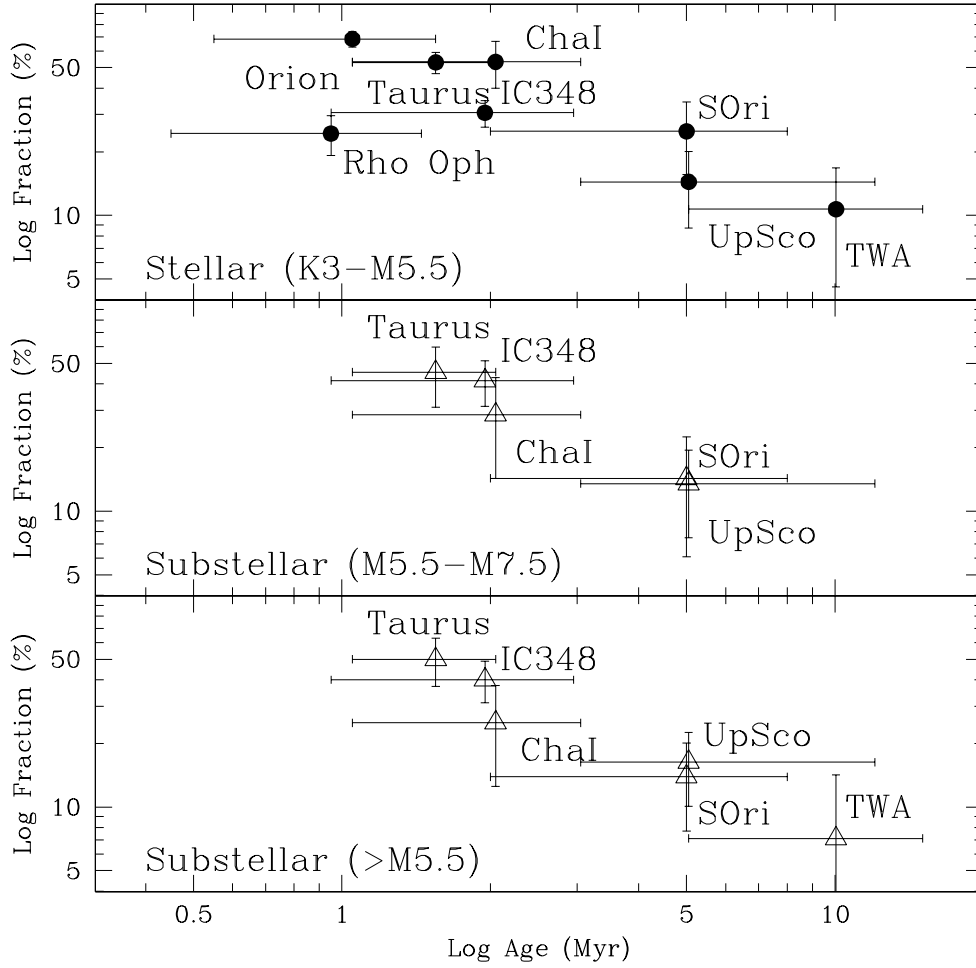


Fig. 6.— Fraction of objects classified as CTT stars or substellar analogs. Solid circles represent the stellar members, whereas the open triangles correspond to the substellar domain (M5.5–M7.5). Note the logarithmic scale.

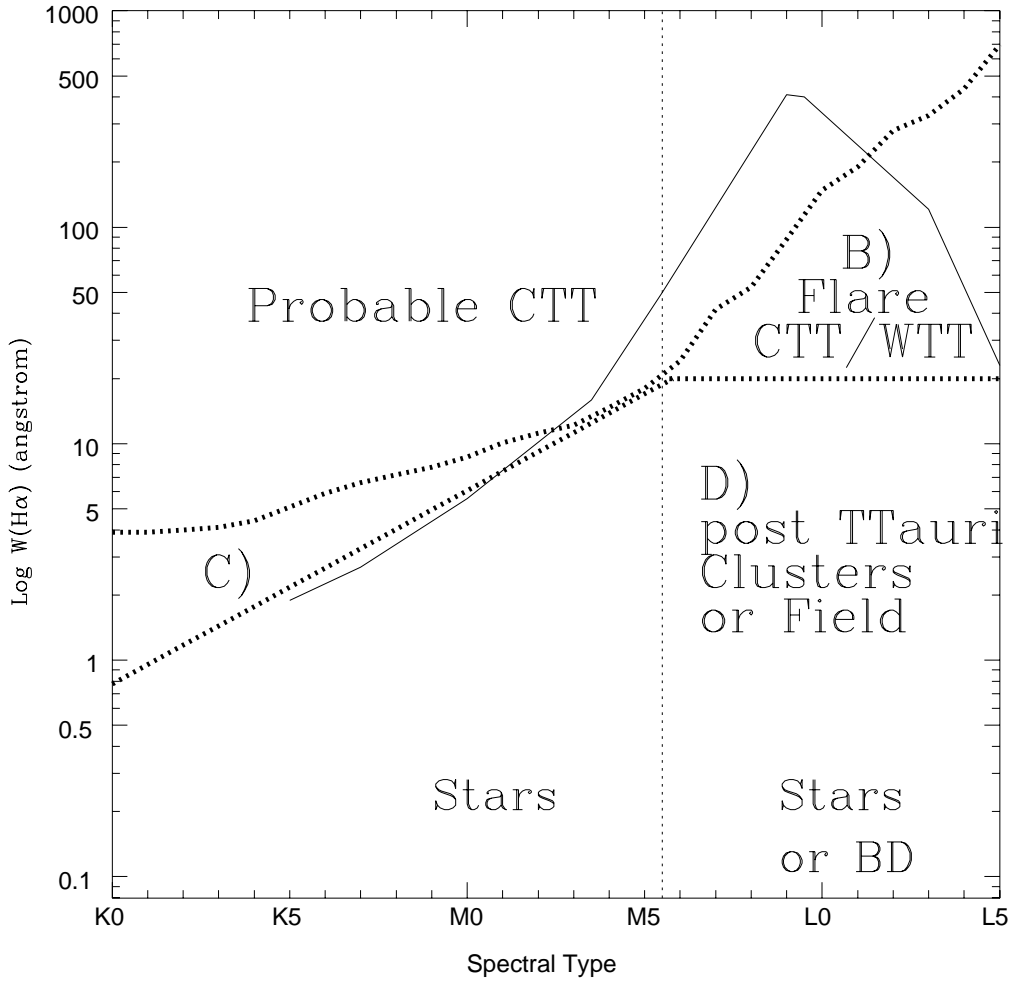


Fig. 7.— Final criteria to classify CTTS and substellar analogs (thick, dotted lines, corresponding to the saturation limit and the maximum activity found in young open clusters). These lines divide the diagram in four very well defined areas. The thin solid line corresponds to the maximum due to flares or very large variability.